New Journal of Physics

CrossMark

PAPER

Spatial confinement causes lifetime enhancement and expansion of vortex rings with positive filament tension

Jan Frederik Totz[1], Harald Engel[1] and Oliver Steinbock[2]

[1] Institut für Theoretische Physik, EW 7-1, TU Berlin, Hardenbergstr. 36, D-10623 Berlin, Germany
[2] Department of Chemistry and Biochemistry, Florida State University, Tallahassee, Florida 32306-4390, USA

E-mail: jantotz@itp.tu-berlin.de

Abstract

We study the impact of spatial confinement on the dynamics of three-dimensional (3D) excitation vortices with circular filaments. In a chemically active medium we observe a decreased contraction rate of such scroll rings and even expanding ones, despite their positive filament tension. All experimentally observed regimes of spatially confined scroll ring evolution are reproduced by full 3D numerical integration of the underlying reaction–diffusion equations. Additionally, we propose a kinematical model that takes into account the interaction of the scroll ring with a no-flux boundary. Its predictions agree quantitatively with data obtained from simulations of the reaction–diffusion model.
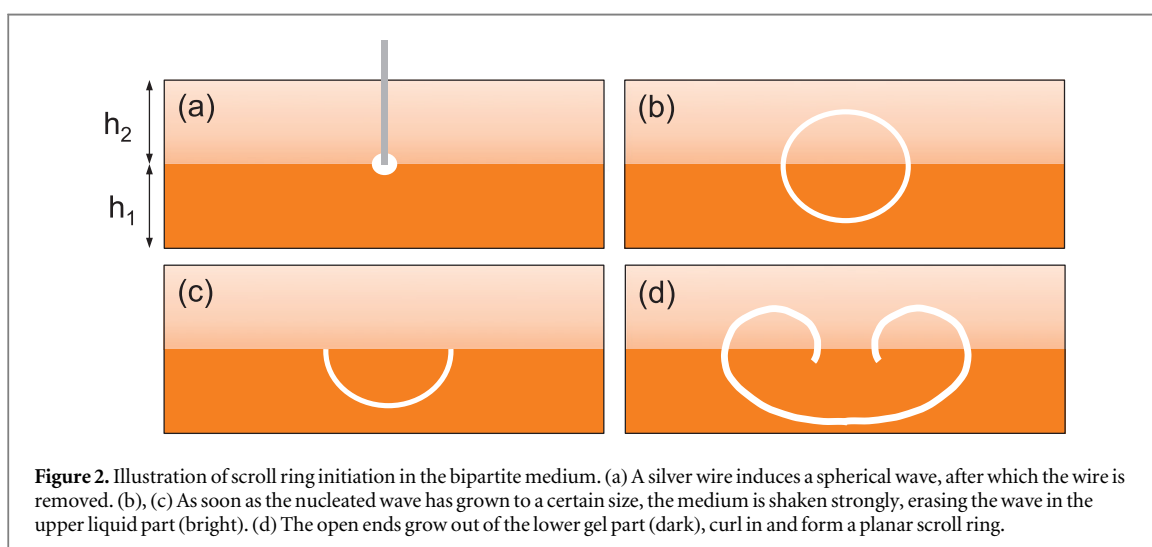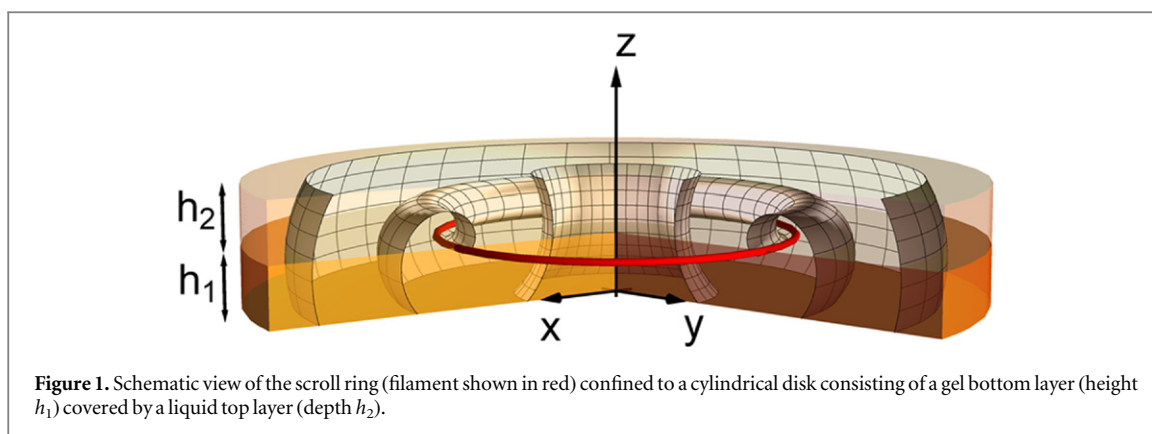
1. Introduction

Confinement effects attract interest across many areas of physics as they generate a wealth of non-intuitive phenomena. One widely studied example is driven Brownian motion in spatial confinement, which exhibits intriguing features such as suppressed diffusion resulting in a violation of the Einstein fluctuation–dissipation relation [1] and hydrodynamically enforced entropic trapping of Brownian particles [2–4]. Phase separation in porous materials leads to layering, freezing, wetting and other phase transitions not found in the bulk system, given that the pore size is on the order of the range of the forces between the confined molecules [5]. Further examples include the efficacy of insect flight [6], vortex-related phenomena such as the onset of turbulence [7] and many others.

Vortex structures exist also in excitable systems including chemical reaction–diffusion media and social waves in honey bee hives [8–10]. Confinement effects in excitable media gained interest, because important examples, such as widely studied multicellular organisms [11, 12] and the human heart [13], measure at most a few vortex wavelengths. Vortices in two-dimensional (2D) excitable systems are rotating spiral waves and exist only above a minimal system size [14, 15]. Their interaction with a no-flux (Neumann) boundary induces a drift of the spiral tip along the wall in which the tip-wall distance is a system-specific value below the pattern wavelength [16–18]. Three-dimensional (3D) generalizations of rotating excitation waves were discovered by Winfree [19], which he termed scroll waves. They organize around a one-dimensional phase singularity called filament. In the limit of small curvature and twist, the local speed of these filaments is proportional to their local curvature [20–23]. In the case of a positive filament tension α, the circular filament of a scroll ring contracts according to a simple square root law [21]. The vortex annihilates in a finite time $R_0^2/(2\alpha)$ where R_0 is the initial filament radius.

For negative α, scroll waves undergo the negative line tension instability that eventually results in a spatio-temporally irregular regime called vortex or Winfree turbulence [20, 24]. This case will not be considered here. We emphasize, however, that confinement can suppress the negative line tension instability of a scroll ring and give rise to the formation of an autonomous boundary-stabilized 3D pacemaker [25].

Experimental and numerical studies on the formation and evolution of free scroll waves and rings have been reported for example in [9, 26–30]. However, the behavior of vortices with positive filament tension near planar

Figure 1. Schematic view of the scroll ring (filament shown in red) confined to a cylindrical disk consisting of a gel bottom layer (height h_1) covered by a liquid top layer (depth h_2).

Figure 2. Illustration of scroll ring initiation in the bipartite medium. (a) A silver wire induces a spherical wave, after which the wire is removed. (b), (c) As soon as the nucleated wave has grown to a certain size, the medium is shaken strongly, erasing the wave in the upper liquid part (bright). (d) The open ends grow out of the lower gel part (dark), curl in and form a planar scroll ring.
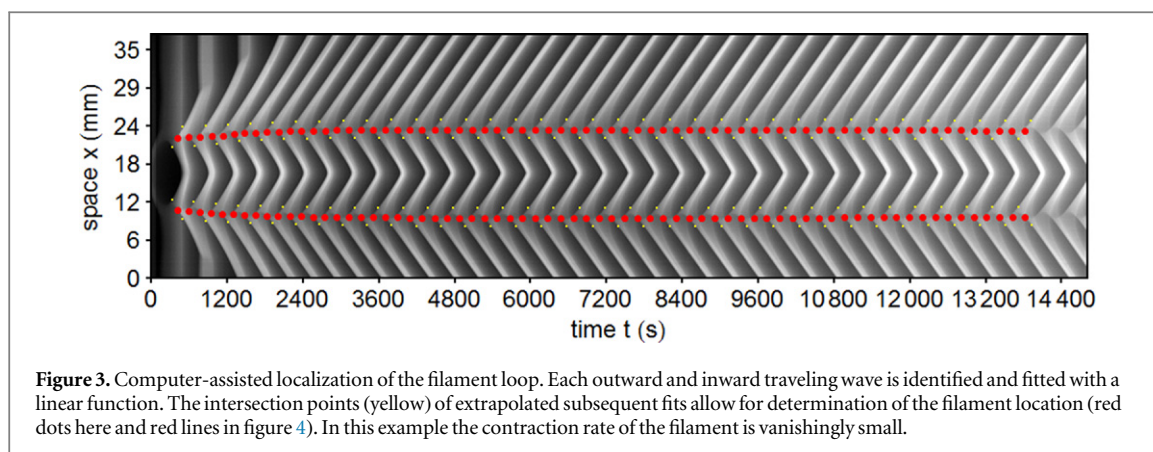
no-flux boundaries has never been studied experimentally. To this end we study the evolution of scroll rings in thin layers of the ferroin-catalyzed Belousov–Zhabotinsky (BZ) reaction (figure 1), [9, 31–33]. We demonstrate experimental evidence that spatial confinement leads to qualitatively new ring dynamics unobtainable in an unbounded medium (section 2). The experimental observations are reproduced in full 3D numerical simulations of the underlying Rovinsky–Aliev reaction–diffusion model [34, 35] (section 3).

Finally we propose a kinematic approach that takes into account the interaction of the scroll ring with a no-flux boundary. The predictions of the kinematical model for the ring dynamics in a phase plane spanned by the filament radius and the distance between filament plane and boundary are in quantitative agreement with data obtained from 3D numerical simulations of the reaction–diffusion model (section 4).

2. Experiments

The reaction takes place in a sealed Petri dish (figure 2). This measure prevents external oxygen from affecting the reaction [36]. Throughout all experiments the same initial reactant concentrations are used: $[H_2SO_4] = 0.16$ M, $[NaBrO_3] = 0.04$ M, [malonic acid] $= 0.04$ M and $[Fe(phen)_3SO_4] = 0.5$ mM. The BZ medium consists of a bottom gel layer (agarose 0.8 % weight/volume) and a top liquid layer. Both layers are prepared from the same concentrations. For these conditions the filament tension of an unbounded scroll ring was previously determined to be as $\alpha = 1.4 \times 10^{-5}$ cm^2 s^{-1}. Curvature-induced filament motion in binormal direction was shown to be vanishingly small [33]. The total medium height is varied in different experiments between 5.2 and 8.0 mm. The spatial extension in the horizontal direction is bounded by the Petri dish diameter (90 mm). Top and bottom boundaries are planar, parallel plexiglass surfaces.

To initiate the scroll ring, we introduce a thin wire of pure silver (99.9%) at the interface of the two layers for about 20 s (figure 2(a)). This decreases the local concentration of inhibitory bromide ions in the direct vicinity of the wire tip. As soon as the developing spherical wave reaches a certain size (figure 2(b)), the system is strongly agitated to spatially homogenize the liquid top layer (figure 2(c)). After the fluid comes to rest again, the

Figure 3. Computer-assisted localization of the filament loop. Each outward and inward traveling wave is identified and fitted with a linear function. The intersection points (yellow) of extrapolated subsequent fits allow for determination of the filament location (red dots here and red lines in figure 4). In this example the contraction rate of the filament is vanishingly small.

unperturbed gel-bound part of the wave extends into it and starts to curl in, thereby nucleating the scroll ring as depicted in figure 2(d)). All scroll rings are initialized in sufficient distance (>30 mm) from the lateral boundaries to exclude their influence.

A charged coupled device camera mounted over the system records transmission image sequences. Grayscale values in the recorded images are proportional to the light transmission integrated across the total height of the active medium [37]. The faint contrast between the blue excited zone and the red refractory wake (corresponding to the oxidized and reduced state of the catalyst, respectively) is enhanced using an additive dichroic filter.

After the experiment, the series of transmission images is reduced to a space time plot by extracting pixels along a line that passes through the center of the circular scroll ring. We developed a code that reconstructs the filament location from the plots based on a method presented in [38]. Each wavefront originating from the filament is identified using a gradient filter and fitted by a linear function. The intersection points of extrapolated fits from a pair of subsequent outward and inward traveling waves allow for a localization of the filament (figure 4). From these data, we can extract the time evolution of the filament radius (figure 5) and the life time of the scroll ring.

Our experiments reveal that the close vicinity of a no-flux boundary can strongly delay the contraction of the filament loop. The scroll ring on figure 4(c) lives longer than the ring shown in figure 4(a) even though its initial radius is smaller. While the larger ring (full circles in figure 5) follows the known square root contraction for the radius [21], the more enduring scroll ring (triangles) decreases slowly in the early stages. Even though the later stages feature a faster decrease, the contraction rate is still below its larger counterpart. This example clearly violates the linear lifetime dependency on R_0^2.
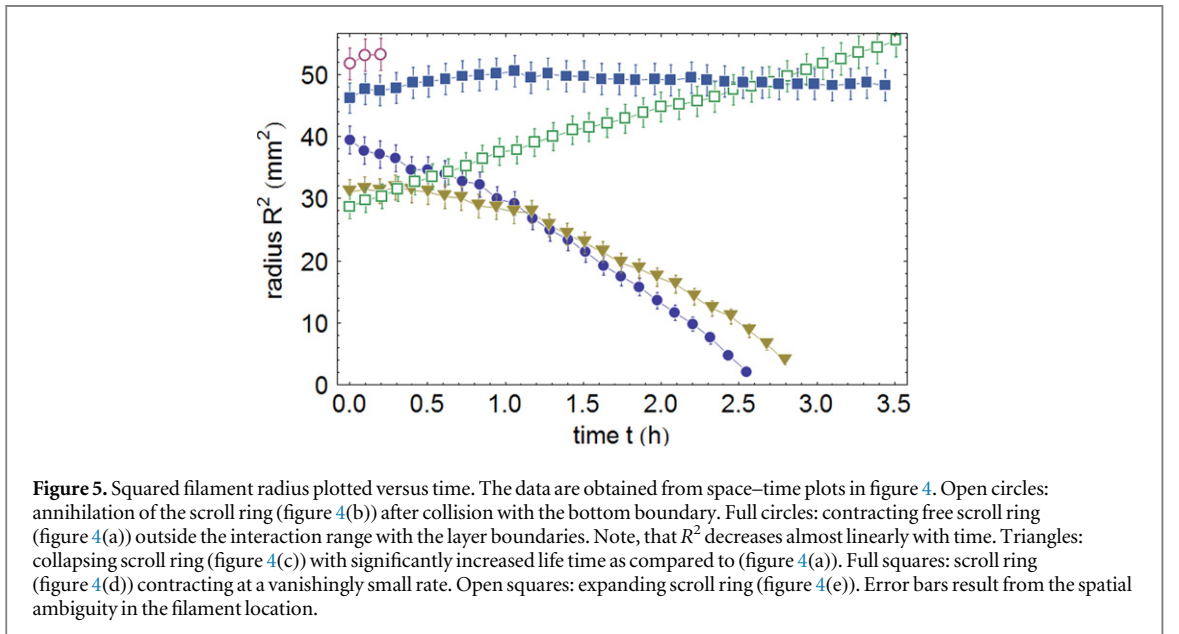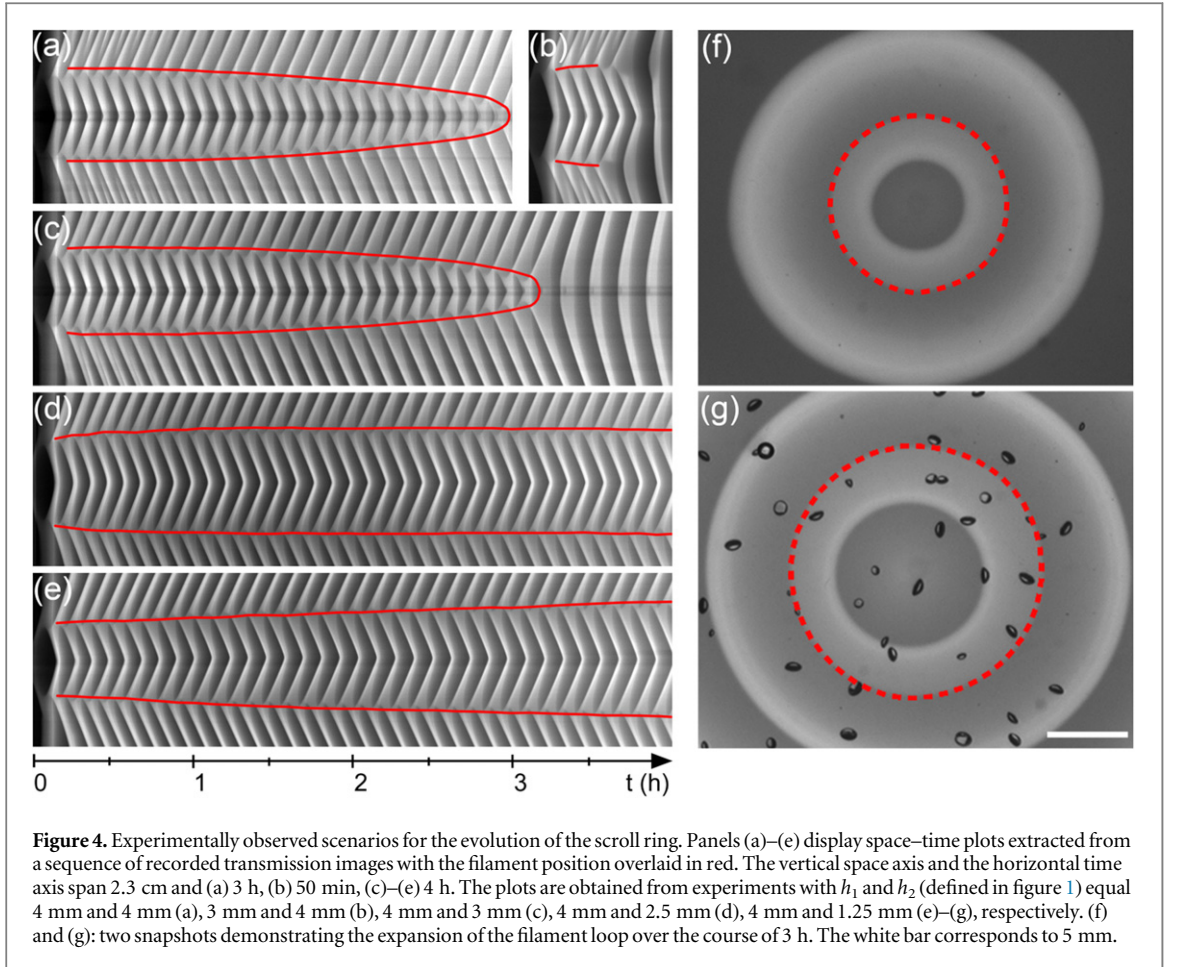
Under stronger spatial confinement we even observe persistent, almost stationary scroll rings (figure 4(d)). In the beginning of the experiment, the ring slightly grows in size until it reaches a maximum after about an hour. Then a nearly vanishing contraction ensues. Over the course of the experiment, the ring lasted for 51 periods and did not collapse.

Moreover, despite of positive filament tension, ring contraction can be superseded by expansion (figure 4(e)). For this example, we choose a small ring in a very thin medium of height 5.25 mm. In contrast to all other cases, this ring expands during the complete experiment and reaches a larger size than of any other ring. Notice the nearly linear increase of R^2 (open squares) for the experimental conditions also shown in figure 4(e). The corresponding increase in R equals about 40% over 3.5 h (figures 4(f), (g)). Eventually the ring breaks apart due to interaction with CO_2 bubbles. These localized inhomogeneities are a product of the BZ reaction and grow in number as well as size over the course of an experiment.

Conversely, the life time of the scroll ring can be drastically reduced by sudden annihilation of the filament with a nearby boundary (figure 4(b)). Instead of an expected lifetime of 3.5 h the ring disappears after 15 min.

3. Numerical simulations based on the Aliev–Rovinsky model

Our experimental results suggest that the interaction of the scroll ring with a confining no-flux boundary is responsible for the observed modifications in the scroll ring dynamics as compared to the spatially unbounded case. In support of this hypothesis, now we study the interaction of a planar scroll ring with a no-flux boundary numerically. To this end we solve the two-component reaction–diffusion model that was developed by Aliev and Rovinsky especially for the ferroin-catalyzed BZ reaction based on the FKN-mechanism [39]. The model is given by the equations

Figure 4. Experimentally observed scenarios for the evolution of the scroll ring. Panels (a)–(e) display space–time plots extracted from a sequence of recorded transmission images with the filament position overlaid in red. The vertical space axis and the horizontal time axis span 2.3 cm and (a) 3 h, (b) 50 min, (c)–(e) 4 h. The plots are obtained from experiments with h_1 and h_2 (defined in figure 1) equal 4 mm and 4 mm (a), 3 mm and 4 mm (b), 4 mm and 3 mm (c), 4 mm and 2.5 mm (d), 4 mm and 1.25 mm (e)–(g), respectively. (f) and (g): two snapshots demonstrating the expansion of the filament loop over the course of 3 h. The white bar corresponds to 5 mm.

Figure 5. Squared filament radius plotted versus time. The data are obtained from space–time plots in figure 4. Open circles: annihilation of the scroll ring (figure 4(b)) after collision with the bottom boundary. Full circles: contracting free scroll ring (figure 4(a)) outside the interaction range with the layer boundaries. Note, that R^2 decreases almost linearly with time. Triangles: collapsing scroll ring (figure 4(c)) with significantly increased life time as compared to (figure 4(a)). Full squares: scroll ring (figure 4(d)) contracting at a vanishingly small rate. Open squares: expanding scroll ring (figure 4(e)). Error bars result from the spatial ambiguity in the filament location.

$$\frac{\partial u}{\partial \tau} = \frac{1}{\epsilon}\left[u - u^2 - \left(2qa\frac{v}{1-v} + b\right)\frac{u-\mu}{u+\mu}\right] + D_u\nabla^2 u,$$

$$\frac{\partial v}{\partial \tau} = u - a\frac{v}{1-v} + D_v\nabla^2 v. \tag{1}$$

Here u and v are proportional to the concentrations of bromous acid and ferriin, respectively. We calculated the values for the parameters a, b, ϵ, q and μ from our recipe concentrations, diffusion coefficients D_u and D_v are

Figure 6. (a) Numerically calculated evolution of scroll rings interacting with a no-flux boundary at $z = 0$ in the parameter plane spanned by the distance from the boundary z and the filament radius R. Different initial conditions are labelled by black dots. The black dotted and black continuous curves are the nullclines $\dot{R} = 0$ and $\dot{z} = 0$ of (3a), respectively. Letters A–E correspond to experimentally observed regimes of ring evolution shown in figure 1. The trajectories of the filament center (thin red lines) calculated from the extended kinematical model (section 4 below) are in quantitative agreement with 3D numerical simulations of the BZ model (thin blue lines). (b) Space–time plot of the persistent ring of case D. Even though it is a transient, the ring configuration appears stationary during the initial 40 periods. Parameter values of the BZ model (1): $\epsilon = 0.47$, $a = 0.018$, $b = 0.00039$, $\mu = 0.00051$, $q = 0.5$, and $D_u = D_v = 2 \times 10^{-5}$ cm^2 s^{-1}. Kinematical parameters (3a): $\alpha = 0.024$ and $\beta = -0.0004$.

the same as in [35, 40]. From 2D simulations of a free spiral wave, we obtain the wavelength $\lambda_{\mathrm{sim}} = 0.56$ cm and the rotation period $T_{\mathrm{sim}} = 372$ s. The corresponding values in the experiment agree very well: $\lambda_{\mathrm{exp}} = 0.58$ cm and $T_{\mathrm{exp}} = 390$ s.

Our full 3D simulations are performed in Cartesian coordinates. Furthermore we used parallelized forward Euler integration with a time step of $d\tau = 0.05$ and a seven-point Laplacian stencil with $dx = 0.001$. Lateral boundaries were at least two wavelengths away from the filament to ensure that their influence was negligible. The filament is determined as the set of points which form the intersection of two level sets of the activator variable u from subsequent time steps.
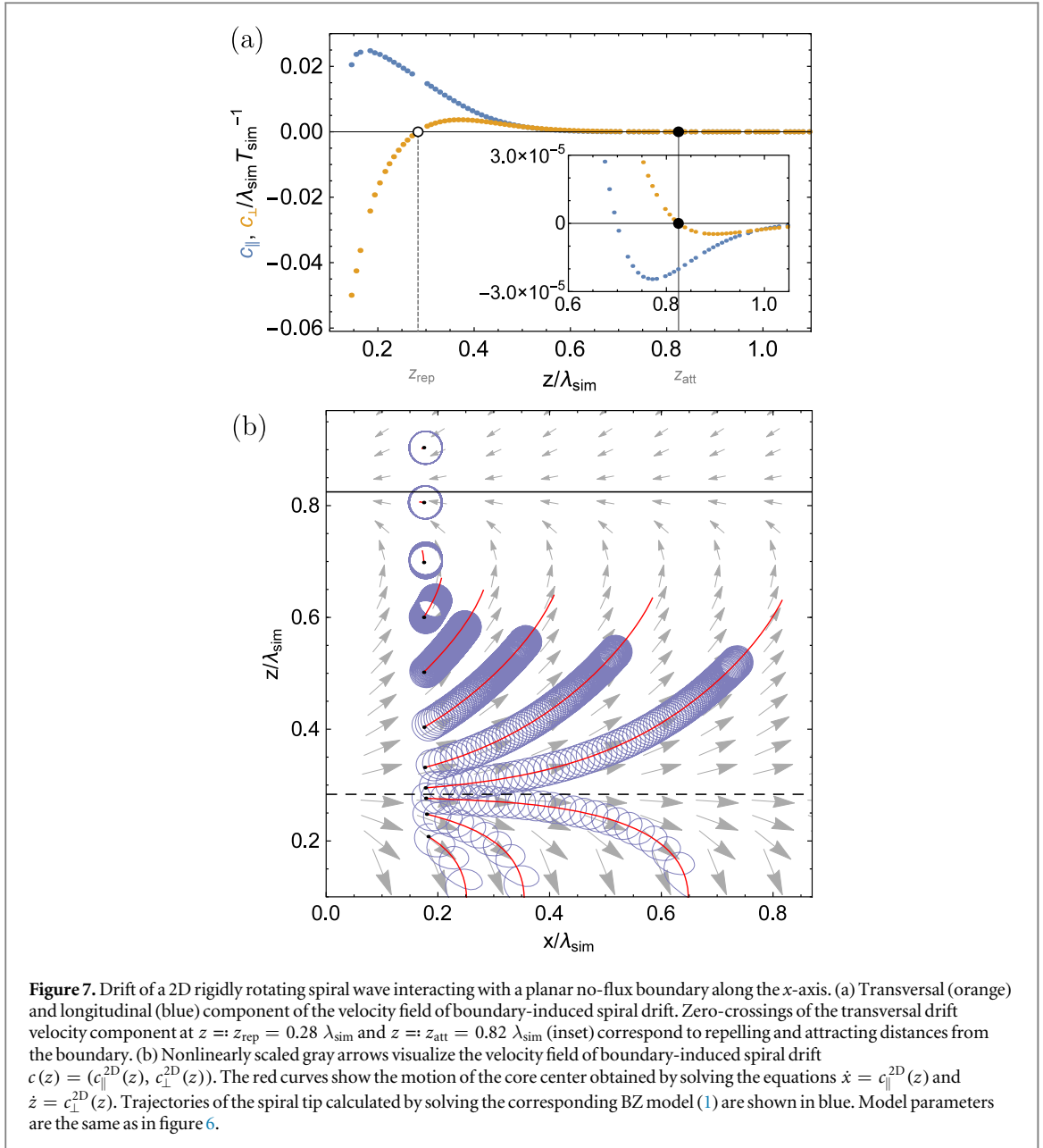
The initiation of the scroll ring mimics the experimental procedure described in figure 2. The scroll rings interact with the bottom no-flux boundary. In simulations with a large cubical grid of edge length $6\ \lambda_{\mathrm{sim}}$ we find unperturbed scroll rings contracting according to the well-known square root dependence $R(t) = \sqrt{R_0^2 - 2\alpha t}$ predicted by Keener *et al* [21]. From a linear fit of R^2 versus time we obtain for the filament tension $\alpha_{\mathrm{sim}} = 0.024\ \lambda_{\mathrm{sim}}^2\ T_{\mathrm{sim}}^{-1}$, which is in very good agreement with the experimentally measured value $\alpha_{\mathrm{exp}} = 0.026\ \lambda_{\mathrm{exp}}^2\ T_{\mathrm{exp}}^{-1}$.

The results of our numerical simulations of the Aliev–Rovinsky equations are summarized in figure 6, where we have plotted trajectories in the R–z-plane with $R(t)$ and $z(t)$ denoting the radius of the filament and the distance of the filament plane from the confining boundary, respectively. Depending on the initial conditions $R_0 = R(t = 0)$ and $z_0 = z(t = 0)$ we find different scenarios for the evolution of the scroll ring. Solutions that show remarkable similarity to regimes observed experimentally are labelled A to E to facilitate the comparison between experimental (figure 4) and numerical (figure 6) results.

4. Kinematical approach

In an unbounded medium scroll rings are non-stationary objects. Their radius, $R(t)$, shrinks or expands with time depending on whether the filament tension α is positive or negative, respectively. Simultaneously, an axisymmetric scroll ring in general drifts along its symmetry axis, $z(t)$. For not too small filament curvature $1/R$ the time evolution of R and z is given by [20, 21, 23]
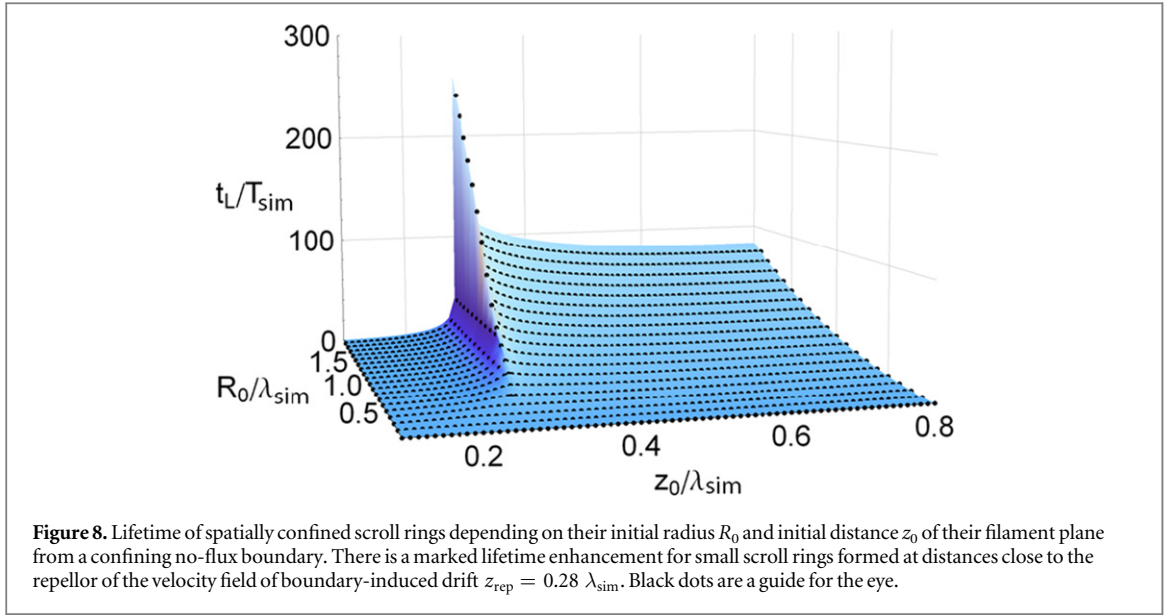
$$
\begin{aligned}
dR/dt &= -\alpha/R, \\
dz/dt &= \beta/R.
\end{aligned}
\qquad (2)
$$

Figure 7. Drift of a 2D rigidly rotating spiral wave interacting with a planar no-flux boundary along the *x*-axis. (a) Transversal (orange) and longitudinal (blue) component of the velocity field of boundary-induced spiral drift. Zero-crossings of the transversal drift velocity component at $z =: z_{rep} = 0.28\,\lambda_{sim}$ and $z =: z_{att} = 0.82\,\lambda_{sim}$ (inset) correspond to repelling and attracting distances from the boundary. (b) Nonlinearly scaled gray arrows visualize the velocity field of boundary-induced spiral drift $c(z) = (c_{\parallel}^{2D}(z), c_{\perp}^{2D}(z))$. The red curves show the motion of the core center obtained by solving the equations $\dot{x} = c_{\parallel}^{2D}(z)$ and $\dot{z} = c_{\perp}^{2D}(z)$. Trajectories of the spiral tip calculated by solving the corresponding BZ model (1) are shown in blue. Model parameters are the same as in figure 6.

In this section we propose an extension of these kinematical equations to account, first, for the interaction of the wave fronts with a single confining no-flux boundary and, second, for the intrinsic interaction between wave fronts forming the ring which becomes important at small radii.

In 2D media, the interaction of a spiral wave with a no-flux boundary has been studied extensively both experimentally and theoretically [16, 41–44]. For a spiral wave a no-flux boundary acts effectively as a resonant periodic perturbation that causes a drift of the spiral core provided the latter is close enough to the boundary. In general the interaction range is smaller than the spiral wavelength, because several wave fronts between spiral core and boundary shield the core region from the perturbing boundary.

Already in 2D, the dependence of the transversal and longitudinal components of the drift velocity field on the distance of the core centre to the boundary *z* is difficult to measure experimentally. Therefore, we calculated the components of the drift velocity field from 2D numerical simulations of the Aliev–Rovinsky model of the ferroin catalyzed BZ which was already used for the full 3D simulations. Figure 7 displays both drift velocity components $c_{\perp}^{2D}(z)$ and $c_{\parallel}^{2D}(z)$ in units of the wavelength, λ_{sim}, and rotation period, T_{sim}, of the unperturbed spiral wave for different distances *z* of the filament plane to the no-flux boundary. The normal velocity component $c_{\perp}^{2D}(z)$ has roots at $z = z_{rep} = 0.28\,\lambda_{sim}$ (dashed line in figure 7(b)) and $z = z_{att} = 0.82\,\lambda_{sim}$. z_{rep} defines a critical distance separating spiral waves that finally annihilate with the boundary from those attracted into a stable regime of constant drift parallel to the boundary at distance z_{att}. Note that for the chosen parameters, the drift velocity at distances comparable to z_{att} is already extremely small. This behavior is expected due to the known exponential decay of the interaction strength between a spiral wave and a no-flux boundary [43, 44].

Figure 8. Lifetime of spatially confined scroll rings depending on their initial radius R_0 and initial distance z_0 of their filament plane from a confining no-flux boundary. There is a marked lifetime enhancement for small scroll rings formed at distances close to the repellor of the velocity field of boundary-induced drift $z_{rep} = 0.28 \, \lambda_{sim}$. Black dots are a guide for the eye.

Based on the 2D simulations, we extend the kinematical model for an unperturbed scroll ring (2) by boundary induced drift fields:

$$dR/dt = -\alpha/R + c_\parallel^{2D}(z) + c_\perp^{2D}(R), \qquad (3a)$$

$$dz/dt = \beta/R + c_\perp^{2D}(z) - c_\parallel^{2D}(R). \qquad (3b)$$

The first term on the right-hand side of equation (3a) describes the contraction of the unconfined scroll ring. Functions $c_\parallel^{2D}(z)$ and $c_\perp^{2D}(z)$ denote the normal and tangential velocity components of the boundary-induced drift of a 2D spiral wave interacting with a planar no-flux boundary discussed above. Velocity components $c_\perp^{2D}(R)$ and $c_\parallel^{2D}(R)$ account for the self-interaction inside very small scroll rings. Note that the cross section of a scroll ring is a spiral wave pair. Across its symmetry axis, a spiral pair solution fulfills the Neumann boundary condition. Therefore to account for self-interaction when the rings are small, we take the already known boundary induced drift field, but replace the distance z with the filament radius R. The minus sign in front of $c_\parallel^{2D}(R)$ is due to the opposite axis orientation in relation to the spiral chirality.

Numerical solutions of the extended kinematical model (red lines in figure 6) agree quantitatively with the filament trajectories obtained from the 3D reaction–diffusion simulations. The dynamics of a free scroll ring with life time $R_0^2/(2\alpha)$ results if the contribution due to filament curvature is dominating over the boundary effects. This is the case when the filament radius is small, or if the distance between filament plane and no-flux boundary leads to comparably small $c_\parallel^{2D}(z)$ values, figures 4(a), 6(A) and figure 5 (filled circles). For sufficiently large filament radii even expanding scroll rings are found in the simulation, as they have been observed in the BZ experiment, figures 4(e), 6(E) and 5 (open squares). Below initial distances $z_0 < z_{rep}$ the scroll ring is pushed by the repellor (dashed line in figure 7(b)) towards the no-flux boundary where it is annihilated before complete collapse. This scenario explains the experimentally observed ring collision with the boundary, figures 4(d), 6(B) and 5 (open circles). For small initial ring radii within $R_0 < 0.6 \, \lambda$, we found that taking into account the interaction between the spiral wave fronts forming the scroll ring improves the agreement between kinematical and numerical results considerably. On the kinematical level, this effect is described by the terms $c_\parallel^{2D}(R)$ and $c_\perp^{2D}(R)$ in (3a), as for self-interaction inside the ring the filament radius R plays the role of the distance z. These two terms are responsible for the drift of the ring along its symmetry axis; they become negligible small for larger core radii. We emphasize that the *transient* ring dynamics in the drift velocity field is crucial in understanding the experimental findings, particularly at the distances near z_{rep}.

From the numerical data obtained within the extended kinematical model (3), we have determined the lifetime of confined scroll rings for different initial sizes R_0 and distances z_0 (figure 8). Obviously, there is a pronounced lifetime enhancement in a range of distances close to z_{rep}. Here, contracting scroll rings evolve with a considerably increased lifetime, figures 4(c), 6(C), and 5 (filled triangles), including almost persistent ones that contract at nearly vanishing rate, figures 4(d), 6(D) and 5 (filled squares). In the latter case, a large scroll ring initially grows and simultaneously departs from the no-flux boundary. This movement in turn weakens the interaction with the boundary and finally causes the ring to contract.

Our results are in line with numerical simulations on interacting mirror-image-like pairs of scroll rings carried out by Bray and Wikswo [40] who observed, for example, a lifetime enhancement of the bound states. This is not surprising, as the interaction within pairs of scroll rings is for symmetry reasons equivalent to the

interaction of one single scroll ring with a nearby planar no-flux boundary. For the same reason, the kinematic model elaborated in our paper is applicable to interacting pairs of scroll rings, too.

5. Summary and conclusion

Taking the ferroin-catalyzed BZ reaction as a representative example, we demonstrate experimentally that axisymmetric scroll rings confined to a thin layer display a rich variety of ring dynamics in excitable media with positive filament tension α. Besides the well-known collapse of the free scroll ring of radius R_0 within finite time $R_0^2/2\alpha$, scroll rings interacting with a planar no-flux boundary exhibit lifetime enhancement up to at least a factor 3. These long living scroll rings act as autonomous 3D pacemakers that last over about four hours during which they change their size by less than 3.5% (figure 4(d)). Moreover, despite of positive filament tension we even found expanding scroll rings.

    We have determined the evolution of the filament depending on the initial size of the ring and the distance from a planar no-flux boundary by full 3D numerical integration of the Aliev–Rovinsky reaction–diffusion model for the ferroin-catalyzed BZ reaction. In these numerical simulations with a single dominating no-flux boundary, we reproduced all experimentally observed regimes of ring evolution.

    We argue that the impact of spatial confinement on scroll ring evolution can be understood within a kinematic approach that combines the intrinsic dynamics of the unconfined scroll ring with boundary-induced drift of spiral waves forming the ring. To check this idea, we propose an extended kinematical model for the dynamics of the confined scroll ring that includes the distance dependent longitudinal and transversal components of the drift velocity field. The quantitative agreement between our kinematical model with the simulations validates our hypothesis that the observed phenomena are explained by a superposition of the intrinsic dynamics of the free scroll ring and boundary-induced spiral drift.

    Recently, we observed stationary boundary-stabilized scroll rings in experiments with the photosensitive BZ reaction [25] as predicted long ago by Winfree [45] for negative line tension. Also in this case, the experimental findings are correctly described by the extended kinematical model.

    The understanding of possible confinement effects on the dynamics of scroll waves is essential for the correct interpretation of experimental data obtained in thin excitable media of the BZ reaction, in cell cultures of cardiac tissue, and many others. Regarding cardiac arrhythmias, for example, it is expected that the dynamics of transmural scroll waves [46, 47] in the comparatively thin atrial tissue will be affected by the interaction with the tissue boundaries. Potentially, overlooked long living transient states can play an important role as quasi-stationary pacemakers, especially when the layer thickness is comparable to the intrinsic wavelength of spiral waves.

Acknowledgments

References

[1] Martens S, Schmid G, Schimansky-Geier L and Hänggi P 2011 *Phys. Rev. E* **83** 051135
[2] Martens S, Straube A V, Schmid G, Schimansky-Geier L and Hänggi P 2013 *Phys. Rev. Lett.* **110** 010601
[3] Dettmer S L, Keyser U F and Pagliara S 2014 *Sci. Instrum. Rev.* **85** 023708
[4] Dettmer S L, Pagliara S, Misiunas K and Keyser U F 2014 *Phys. Rev. E* **89** 062305
[5] Gelb L D, Gubbins K E, Radhakrishnan R and Sliwinska-Bartkowiak M 1999 *Rep. Prog. Phys.* **62** 1573
[6] Rayner J, Thomas A, Rayner J and Thomas A 1991 *Phil. Trans. R. Soc. B* **334** 107
[7] Doligalski T, Smith C and Walker J 1994 *Ann. Rev. Fluid Mech.* **26** 573
[8] Agladze K and Steinbock O 2000 *J. Phys. Chem.* **104** 9816
[9] Bánsági T and Steinbock O 2006 *Phys. Rev. Lett.* **97** 198301
[10] Kastberger G, Schmelzer E and Kranner I 2008 *PLoS One* **3** e3141
[11] Steinbock O, Siegert F, Müller S and Weijer C 1993 *Proc. Natl Acad. Sci.* **90** 7332
[12] Zykov V S, Oikawa N and Bodenschatz E 2011 *Phys. Rev. Lett.* **107** 254101
[13] Cherry E and Fenton F 2011 *J. Theor. Biol.* **285** 164
[14] Hartmann N, Bär M, Kevrekidis I G, Krischer K and Imbihl R 1996 *Phys. Rev. Lett.* **76** 1384
[15] Yang J and Zhang M 2006 *Phys. Lett. A* **352** 69
[16] Brandtstädter H, Braune M, Schebesch I and Engel H 2000 *Chem. Phys. Lett.* **323** 145
[17] Schebesch I and Engel H 1999 *Phys. Rev. E* **60** 6429
[18] Zemlin C, Mukund K, Wellner M, Zaritsky R and Pertsov A 2005 *Phys. Rev. Lett.* **95** 098302
[19] Winfree A T 1973 *Science* **181** 937–9
[20] Biktashev V, Holden A and Zhang H 1994 *Phil. Trans. R. Soc. A* **347** 611
[21] Keener J and Tyson J 1992 *SIAM Rev.* **34** 1

[22] Panfilov A V, Rudenko A N and Krinsky V I 1986 *Biofizika* **31** 850

[23] Panfilov A and Rudenko A 1987 *Physica* D **28** 215

[24] Bánsági T and Steinbock O 2007 *Phys. Rev.* E **76** 045202

[25] Azhand A, Totz J F and Engel H 2014 *EPL* **108** 10004

[26] Storb U, Neto C R, Bär M and Müller S C 2003 *Phys. Chem. Chem. Phys.* **5** 2344–53

[27] Alonso S, Sagués F and Mikhailov A S 2003 *Science* **299** 1722–5

[28] Alonso S, Sagués F and Mikhailov A S 2006 *J. Phys. Chem.* **A110** 12063–71

[29] Luengviriya C, Storb U, Lindner G, Müller S C, Bär M and Hauser M J B 2008 *Phys. Rev. Lett.* **100** 148302

[30] Dähmlow P, Alonso S, Bär M and Hauser M J B 2013 *Phys. Rev. Lett.* **110** 234102

[31] Linde H and Engel H 1991 *Physica* D **49** 13–20

[32] Amemiya T, Kettunen P, Kádár S, Yamaguchi T and Showalter K 1998 *Chaos* **8** 872

[33] Jiménez Z A and Steinbock O 2012 *Phys. Rev.* E **86** 306205

[34] Rovinskii A B and Zhabotinskii A M 1984 *J. Phys. Chem.* **88** 6081

[35] Aliev R and Rovinskii A 1992 *J. Phys. Chem.* **96** 732

[36] Taylor A F, Johnson B R and Scott S K 1999 *Phys. Chem. Chem. Phys.* **1** 807–11

[37] Müller S C, Plesser T and Hess B 1987 *Physica* D **24** 87–96

[38] Pertsov A, Vinson M and Müller S C 1993 *Physica* D **63** 233–40

[39] Field R J, Koros E and Noyes R M 1972 *J. Am. Chem. Soc.* **94** 8649–64

[40] Bray M A and Wikswo J P 2003 *Phys. Rev. Lett.* **90** 238303

[41] Ermakova E A, Pertsov A M and Shnol E E 1989 *Physica* D **40** 185–95

[42] Gómez Gesteira M, Muñuzuri A P, Pérez Muñuzuri V and Pérez Villar V 1996 *Phys. Rev.* E **53** 5480–3

[43] Aranson I S, Kramer L and Weber A 1991 *Physica* D **53** 376

[44] Aranson I S, Kramer L and Weber A 1993 *Phys. Rev.* E **47** 3231–41

[45] Nandapurkar P J and Winfree A T 1989 *Physica* D **35** 227

[46] Cherry E M and Fenton F H 2008 *New J. Phys.* **10** 125016

[47] Biktasheva I, Dierckx H and Biktashev V 2015 *Phys. Rev. Lett.* **144** 068302